Published in final edited form as:
Biochemistry. 2009 May 5; 48(17): 3787–3794. doi:10.1021/bi802070j.

Constitutively Active Akt Inhibits Trafficking of Amyloid Precursor Protein and Amyloid Precursor Protein Metabolites through Feedback Inhibition of Phosphoinositide 3-Kinase†

Diana W. Shineman, **Aleksandra S. Dain**, **Minkyu L. Kim**, and **Virginia M.-Y. Lee***
Department of Pathology and Laboratory Medicine, Center for Neurodegenerative Disease Research, University of Pennsylvania School of Medicine, Philadelphia, Pennsylvania 19104

Abstract

Amyloid-*β* (A*β*) peptides, generated through sequential proteolytic cleavage of amyloid precursor protein (APP), aggregate to form amyloid plaques in Alzheimer's disease (AD). Understanding the regulation of A*β* generation and cellular secretion is critical to our understanding of AD pathophysiology. In the present study, we examined the role of the insulin/insulin-like growth factor-1 (IGF-1) signaling pathway in regulating APP trafficking and A*β* secretion. Previous studies have demonstrated that insulin or IGF-1 stimulation can increase A*β* and APP secretion in a phosphoinositide 3-kinase (PI3K) dependent manner. To expand upon these studies and better understand the molecular targets responsible for alterations in APP secretion, we constitutively activated Akt, a downstream component of the insulin/IGF-1 signaling pathway. Counterintuitively, constitutively active Akt (myr-Akt) overexpression produced an opposite effect to insulin/IGF-1 stimulation and inhibited secretion of APP and APP metabolites in multiple cell lines. Myr-Akt overexpression also resulted in increased APP protein stability. Since the insulin/IGF-1 signaling pathway is tightly regulated by feedback inhibition pathways, we hypothesized that myr-Akt overexpression may be inducing feedback inhibition of PI3K, resulting in impaired APP trafficking. In support of this hypothesis, myr-Akt acted at a known node of PI3K inhibition and decreased insulin receptor substrate 1 (IRS1) protein levels. Our studies provide further support for PI3K as a modulator of APP trafficking and demonstrate that overactivation of the insulin/IGF-1 signaling pathway may result in feedback inhibition of PI3K through IRS1 and reduce APP trafficking and A*β* secretion.

Amyloid plaques, one of the major pathological hallmarks of Alzheimer's disease (AD),[1] are composed mainly of amyloid-*β* (A*β*) peptides produced from the sequential proteolytic cleavage of amyloid precursor protein (APP). APP is a type I transmembrane domain protein that is secreted through the trans Golgi network (TGN) to the plasma membrane where it can be reinternalized into endosomes and ultimately degraded by the lysosome (1). APP cleavage occurs constitutively throughout the secretory pathway. Cleavage of APP by α-secretase generates secreted N-terminal APPα (sAPPα) ectodomain and C83 C-terminal fragment (CTF), while *β*-secretase cleavage of APP generates secreted N-terminal APP*β* (sAPP*β*) and C99 CTF. The C99 CTF are then cleaved by *γ*-secretase at one of several proteolytic sites, thereby generating A*β* peptides of varying lengths. The most common peptide produced is A*β*1–40, followed by A*β*1–42 (2–5).

†These studies were supported by a grant from the NIH (AG-11542).

*To whom correspondence should be addressed. Tel: 215-662-6427. Fax: 215-349-5909. vmylee@mail.med.upenn.edu.

[1]Abbreviations: APP, amyloid precursor protein; A*β*, amyloid-*β*; AD, Alzheimer's disease; PI3K, phosphoinositide 3-kinase; GSK3, glycogen synthase kinase 3; IGF-1, insulin-like growth factor-1; IRS1, insulin receptor substrate 1.

APP cleavage reactions are dependent on subcellular localization. Cleavage by α-secretase occurs at the plasma membrane as well as in intracellular vesicles budding from the TGN (6). *β*-Secretase cleavage of APP occurs in the TGN as well as in endosomes following internalization of APP from the plasma membrane (7,8). *γ*-Secretase cleavage is thought to occur at any point along the secretory pathway, resulting in the generation of A*β* in intracellular vesicles (9,10). These vesicles containing sAPPs (i.e., both sAPPα and sAPP*β*) and A*β* can then fuse with the plasma membrane to release their contents into the extracellular space. While intracellular pools of these secreted products have been detected, the levels are normally minimal compared to the extracellular pool (11).

The insulin/insulin-like growth factor-1 (IGF-1) signaling pathway has previously been shown to regulate secretion of APP and A*β*. Stimulation of insulin/IGF-1 receptor by ligand binding results in activation of downstream signaling cascades including activation of phosphoinositide 3-kinase (PI3K) (12). When activated, the insulin/IGF-1 receptor induces dimerization and autophosphorylation, facilitating binding and tyrosine phosphorylation of adaptor proteins, such as insulin receptor substrate 1 (IRS1). IRS1 binds to the regulatory subunit of PI3K, allowing for membrane location and activation of downstream proteins. Activation of PI3K mediates the downstream effects of insulin/IGF-1 signaling such as Akt activation and subsequent regulation of numerous targets, including glycogen synthase kinase 3 (GSK3) inhibition and mammalian target of rapamycin (mTOR) (12). PI3K can also activate Akt-independent pathways such as atypical protein kinase C (aPKC) *λζ* to mediate other downstream signaling responses (13,14).

Previous studies have demonstrated that insulin and IGF-1 stimulation can increase APP secretion in a PI3K-dependent manner (15–17). In addition, inhibition of PI3K activity, even in the absence of stimulation, decreases APP trafficking and secretion (16,18). To expand on these previous studies and further understand the mechanism downstream of insulin/IGF-1-induced stimulation of APP secretion, we overexpressed constitutively active Akt (myr-Akt) in multiple cell lines. Surprisingly, we found that chronic activation of Akt produced the opposite result to that seen with insulin/IGF-1 stimulation and reduced trafficking and secretion of APP and APP metabolites. Given that the insulin signaling pathway is carefully regulated through multiple points of feedback inhibition, we hypothesized that the effects of myr-Akt on APP trafficking may be mediated through feedback inhibition of PI3K. Indeed, levels of IRS1, an adaptor protein required for PI3K activation and a major node for feedback inhibition, were significantly reduced following myr-Akt overexpression. Together, these results suggest that overactivation of Akt could negatively regulate APP trafficking and lead to decreased secretion and intracellular accumulation of A*β*.

EXPERIMENTAL PROCEDURES

Materials

APPwt-pcDNA3.1 and APPsw-pcDNA3.1 constructs have been described previously (19). Aktwt-pUSE, myr-Akt-pUSE, and pUSE empty vector constructs were obtained from Morris Birnbaum (University of Pennsylvania, Philadelphia, PA). Cyclohexamide was purchased from Sigma-Aldriich (St. Louis, MO). *γ*-Secretase inhibitor X (L-685,458) and PI3K inhibitor LY-294002 were purchased from EMD Biosciences (Gibbstown, NJ).

Tissue Cell Culture

QBI293 cells (a subclone derived from HEK293 cells), CHO (Chinese hamster ovary) cells, and mouse neuroblastoma N2a cells were grown in DMEM 4.5 g/L glucose (Invitrogen, Carlsbad, CA), 10% fetal bovine serum, L-glutamine, and penicillin/streptomycin at 37 °C and 5% CO_2 according to standard protocols. QBI293 cells were transfected at 90%

confluence using lipofectamine 2000 (Invitrogen, Carlsbad, CA) following the manufacturer's protocols. Both CHO and N2a cells were transfected using the AMAXA nucleofector system (Gaithersburg, MD) according to the manufacturer's protocol. Where indicated, cells were treated with 50 μg/mL cyclohexamide, 500 μM chloroquine, 50 mM NH_4Cl, 1 μM γ-secretase inhibitor X, or 50 μM PI3K inhibitor LY-294002. For measurements of protein stability, QBI293 cells were transfected with indicated constructs for 24 h, after which cells were treated with cyclohexamide and harvested at indicated time points.

Harvesting Cell Lysate and Media

Following transfections or cell treatment paradigms, conditioned media were collected and supplemented with 1 μg/mL protease inhibitor cocktail and 0.5 mM PMSF and centrifuged at 13000*g* for 10 min to pellet cell debris. Supernatant was used for Western blot or ELISA analysis of conditioned media. Cells were washed twice with ice-cold PBS and lysed in RIPA buffer (0.5% sodium deoxycholate, 0.1% SDS, 1% NP-40, 5 mM EDTA, pH 8.0, 1 μg/mL protease inhibitor cocktail, and 0.5 mM PMSF). Cell lysates were sonicated and spun at 13000*g* for 25 min. For DEA-RIPA sequential extraction, 2% diethanolamine (DEA) in 50 mM NaCl buffer was added to the cells. Cells were scraped into sample tubes and homogenized with a Dounce homogenizer and spun at 100000*g*. Supernatant was neutralized with 10% volume of 0.5 M Tris, pH 6.8, and the pellet was sonicated in RIPA buffer as described above. Protein amount was determined by BCA assay.

ELISA Measurements

Sandwich ELISA measurements of Aβ were performed as described previously (20). Briefly, conditioned media or RIPA lysate was added to plates coated with Ban50 as the capture antibody. After overnight incubation at 4 °C, plates were washed and incubated with HRP-conjugated BA27 (Aβ40 specific) or BC05 (Aβ42 specific) antibodies for 4 h at room temperature followed by chemiluminescence detection. Values were calculated by comparison to standard curves of Aβ40 and Aβ42 synthetic peptides (Bachem, Torrance, CA). For ELISA measurements of sAPPα, a sandwich ELISA was performed using LN27 antibody (21) as the capture and Ban50-HRP conjugate as reporting antibody.

Western Blot Analysis

Equal amounts of protein were loaded and run on a 7.5% SDS–PAGE Tris–glycine gel, transferred to nitrocellulose membrane, blocked in 5% milk, and probed with indicated antibodies. Immunoreactive bands were identified by enhanced chemiluminescence (ECL). For detection of full-length APP, we used either 5685 or a goat polyclonal antibody raised to the N-terminus of APP (Karen) (22). For N2a cells, human-specific Ban50 antibody (Takeda) was used to eliminate immunoreactivity from mouse APP. For detection of sAPPα, conditioned media were collected and supplemented with PMSF and protease inhibitors and were run directly on 7.5% SDS–PAGE and probed with Ban50 antibody. For secreted sAPPβ_{sw} measurements, conditioned media were immunoprecipitated with a goat anti-APP antibody (Karen) (22) and protein A/G beads overnight at 4 °C. Immunoprecipitates were run on 7.5% SDS–PAGE gel and immunoblotted with an antibody specific to the C-terminus of sAPPβ_{sw} (no. 54) (23). For detection of C-terminal fragments, equal protein amounts were loaded on a 15% Tris–tricine gel and probed with a rabbit polyclonal antibody raised to the C-terminus of APP (5685) (23). To verify consistent loading on Western blots of cell lysate, the bottom half of the blot was probed with an anti-α-tubulin antibody (Sigma) or anti-β actin antibody (Sigma) where indicated. Western blots were quantified using Fujifilm multigauge software v2.3. Relative pixel density was calculated for each band following background subtraction.

Statistical Analysis

Data are expressed as mean ± SD. For statistical analysis, unpaired Student's *t* test was performed using Microsoft Excel. Statistical significance was set to $p < 0.05$.

RESULTS

Myr-Akt Expression Increases APP Levels and Decreases Secretion of APP Metabolites

To test the effects of activating downstream components of the insulin/IGF-1 receptor activation on APP metabolism, we overexpressed constitutively active Akt (myr-Akt) in QBI293 cells, a subclone derived from HEK293 cells. Expression of wild-type APP (APPwt) with myr-Akt resulted in an increase in full-length APP levels (indicated by upper arrow) as well as an increase in a lower molecular weight species (indicated by starred arrow) that is immunoreactive with APP N-terminal antibody (Figure 1A). Expression of APP with wild-type Akt (wtAkt) did not alter APP levels when compared to empty vector (vec). To verify the proper activation of myr-Akt following transfection, the phosphorylation state of Akt was analyzed. As expected, cells overexpressing myr-Akt demonstrated increased phophorylation as compared to vector alone or wtAkt expression, as assessed by Western blot (Figure 1A). Further, myr-Akt expression resulted in increased inhibitory phosphorylation of GSK-3, indicating the construct is functioning as expected to activate downstream signaling pathways (data not shown). Similar results were found with coexpression of APP containing the Swedish familial mutation (APPsw) as opposed to APPwt (data not shown). Since no significant difference between APPwt and APPsw was found, APPsw was used in many cases as this mutation increases *β*-secretase cleavage and results in elevated A*β* generation, allowing for easier detection by ELISA.

To determine the identity of the APP immunoreactive lower molecular weight band, QBI293 cells transfected with APPsw and either myr-Akt or wtAkt were sequentially extracted with DEA, a buffer that allows for the extraction of soluble sAPPs but not the membrane-anchored full-length APPsw. As expected, sAPPα, the lower molecular weight bands indicated by the starred arrow, but not full-length APP, was extracted with DEA buffer and was recognized by both an N-terminal APP antibody as well as a cleavage site specific sAPPα antibody (2B3) (Figure 1B). α-Tubulin Western blot is shown as a loading control. Full-length APP (indicated by upper arrow) and sAPPα (starred arrow) were also detected in the RIPA fraction and were significantly elevated with myr-Akt expression. Therefore, myr-Akt expression increased levels of both full-length APP and sAPPα in the cell lysate. wtAkt expression did not alter APPsw or sAPPα levels compared to vector expression. While we are specifically measuring sAPPα, sAPP*β* levels may also be elevated in the cell lysate. Since *β*-cleavage of APP occurs at a much lower frequency than α-cleavage in non-neuronal cells, the levels in the lysate were difficult to measure with available antibodies.

In addition to the increase in sAPP and APP in the cell lysate, intracellular A*β* levels were also increased in cells expressing myr-Akt as determined by sandwich ELISA, even when normalized to APP (Figure 1C). However, extracellular levels of both A*β*40 and A*β*42 levels were significantly reduced with myr-Akt expression (Figure 1D) as were extracellular levels of sAPPα as measured by sandwich ELISA (Figure 1E). Therefore, it appears that secretion of APP metabolites is impaired with myr-Akt expression, causing an abnormal intracellular accumulation of both A*β* and sAPPs.

To determine if these effects could be demonstrated in other cell types, we overexpressed APP with either empty vector or myr-Akt (myr) in CHO cells. Consistent with our findings in QBI293 cells, APPsw levels in the cell lysate were increased with myr-Akt expression, while levels of sAPPα and sAPP*β*sw in conditioned media were decreased (Figure 2A). Further, extracellular A*β*40 and A*β*42 levels in conditioned media from CHO cells were

decreased with myr-Akt expression (Figure 2B). Similar results were found in N2a cells, a neuroblastoma cell-line, although these cells were more difficult to transfect and expressed lower levels of APP. APP levels were increased with myr-Akt expression (Figure 2C). Extracellular Aβ40 levels were also significantly reduced with myr-Akt expression in N2a cells (Figure 2D). Aβ42 levels were too low to reliably measure from these cells.

Myr-Akt Expression Does Not Significantly Alter Cleavage of APP

Though constitutive activation of Akt appears to affect secretion of APP metabolites, we wanted to assess any effect myr-Akt may have on the enzymatic cleavage of APP. Myr-Akt overexpression increased both the β-cleaved C-terminal fragment of APP (C99) and α-cleaved fragment (C83) when compared to empty vector (Figure 3A). The increase in CTFs was proportional, and there was no significant difference in the ratio of C83/C99 between myr-Akt and vector expression paradigms (Figure 3B), suggesting that neither α- nor β-secretase cleavage is preferentially modified. In addition, the ratio between C83 and C99 was largely unchanged when myr-Akt was coexpressed with APPsw as well (data not shown). Therefore, myr-Akt expression does not appear to significantly alter APP α- or β-cleavage reactions.

To test if the increase in CTFs reflects the increase in the upstream substrate, APP, or an inhibition of γ-secretase, QBI293 cells were treated with a γ-secretase inhibitor. Chemical inhibition of γ-secretase did not affect the ability of myr-Akt to increase the levels of CTFs (Figure 3C). Therefore, our studies support the hypothesis that myr-Akt does not act to alter CTFs through regulation of γ-secretase cleavage of APP.

Myr-Akt Expression Increases APP Protein Stability through Reduced Lysosomal Degradation of APP

To determine the mechanism of increased full-length APP levels seen with myr-Akt expression, APP levels were analyzed at indicated time points following cyclohexamide treatment. Myr-Akt expression significantly increased APP protein stability, while wt-Akt was similar to vector control (Figure 4A,B). Since myr-Akt expression reduced trafficking and secretion of APP metabolites, we hypothesized that the increase in APP protein stability could be due to decreased trafficking of APP to the lysosome. To test this hypothesis, we analyzed myr-Akt's effects on APP levels in the presence of lysosomal inhibitor treatment (NH_4Cl or chloroquine). Myr-Akt normally increases APP levels. Under conditions of lysosomal inhibition, APP levels were increased at baseline but were not further increased with myr-Akt expression (Figure 4C). These data suggest that myr-Akt increases APP through inhibition of the lysosomal degradation pathway. It is tempting to speculate that myr-Akt increases APP protein stability by decreasing vesicular trafficking of APP to the lysosome. However, the precise mechanism of myr-Akt's effect on APP levels is unclear. Further investigation is warranted to confirm the role of the lysosome in this paradigm and to better understand the mechanism of myr-Akt action.

Myr-Akt Overexpression May Act through Feedback Inhibition of PI3K To Alter APP Trafficking

Previous studies have shown that PI3K inhibition reduces APP secretion in a similar manner to myr-Akt overexpression (18). Faced with these counterintuitive results, we hypothesized that myr-Akt overexpression may be causing feedback inhibition of PI3K. Feedback inhibition pathways mediated through Akt are well-known and have been demonstrated previously (24,25). First, to directly test if PI3K inhibition produces effects similar to myr-Akt expression in our system, we treated QBI293 cells expressing APP with the PI3K inhibitor LY-294002 (LY). LY treatment increased APP levels (Figure 5A). In addition, extracellular Aβ40 and Aβ42 levels were significantly reduced following LY treatment

(Figure 5B) as were sAPPα levels in conditioned media (Figure 5C), as determined by ELISA.

Previously described feedback inhibition pathways for the insulin signaling pathway involve regulation of IRS1 protein levels (25,26). IRS1 is a scaffold protein that binds to the regulatory subunit of PI3K, allowing for localization and activation of the enzyme. IRS1 can be phosphorylated and targeted for degradation by feedback inhibition pathways, thereby inhibiting PI3K. Indeed, we found that IRS1 protein levels were significantly reduced following myr-Akt expression (Figure 5D). These results were very reproducible, and quantification of multiple experiments demonstrated a statistically significant reduction in IRS1 (Figure 5E). These results are consistent with a feedback inhibition hypothesis.

DISCUSSION

In this study, we show that constitutively active Akt overexpression reduced trafficking of APP, resulting in reduced secretion of APP metabolites and decreased degradation of APP by the lysosome (Figure 6). While somewhat counterintuitive, these effects can be explained by feedback inhibition of PI3K, as PI3K inhibition produced similar results. Consistent with a feedback inhibition hypothesis, myr-Akt expression resulted in a significant decrease in IRS1 protein levels. No significant changes in the ratio of APP cleavage products were noted, indicating that APP cleavage reactions were largely unmodified.

Our studies suggest that overactivation of Akt results in feedback inhibition of PI3K through reduced IRS-1 protein levels. IRS1 can be both positively and negatively regulated by a number of different pathways (26). While tyrosine phosphorylation is considered activating, serine phosphorylation inhibits the activity of IRS1, either by targeting IRS1 for degradation or by disrupting binding and inhibiting activation of PI3K. The feedback inhibition pathway has been well described, and other studies have shown functional consequences of this feedback inhibition *in vivo.* For example, chronic Akt activation has been shown to induce feedback inhibition of PI3K activity through proteasome-dependent degradation of IRS-1 and through inhibition of transcription of IRS-1 and IRS-2 (24). These effects were rescued by constitutively active PI3K overexpression. In our studies, however, we do not know how IRS1 phosphorylation is modified or if the reduction in IRS1 occurs at the protein or mRNA level or both. Future studies include directly measuring IRS1 phosphorylation using phospho-specific antibodies and measuring IRS1 mRNA levels following myr-Akt expression. It would also be important to test if overexpression of constitutively active PI3K constructs can rescue the impairment in APP trafficking seen with chronic Akt activation and if PI3K activity in the cell is globally reduced.

The molecular feedback pathway caused by chronic Akt activation is also unclear. The mammalian target of rapamycin (mTOR) is downstream of Akt and can phosphorylate IRS1 on serine residues, targeting it for degradation (27). Using rapamycin to inhibit mTOR activity should block this feedback pathway; however, we were unable to consistently block the effects of myr-Akt expression with rapamycin treatment (data not shown). Therefore, it appears that other signal transduction pathways are involved that mediate effects of myr-Akt on IRS1. IRS1 activity could be negatively regulated by a number of different kinases, including JNK (28), PKCδ (29), IKKB (30), ERK (31), and PKCθ (32). It would be interesting to test if inhibitors of each of these kinases could block the effects of myr-Akt expression on APP.

Since there are extensive pathways in place that can inhibit activation of IRS1 and the insulin receptor signaling pathway, this begs the question as to why these negative feedback pathways exist. Since this pathway is involved in cell growth, activation must be carefully

controlled to prevent uncontrolled cell growth and cancer. In fact, many components of the insulin signaling pathway, such as IRS1 (33) and Akt (34), have been demonstrated to be overactivated in various cancers.

While this study provides further support for PI3K in regulating APP trafficking, the mechanism of this regulation is currently unknown. Since Akt overactivation does not produce any stimulatory activity on APP trafficking, we hypothesize the effects of PI3K on APP trafficking to be Akt independent. In support of this hypothesis, overexpression of dominant negative Akt constructs did not result in any changes in APP levels or in secretion of APP metabolites (data not shown). Given what is known about PI3K-dependent trafficking of GLUT4 to the plasma membrane, it is tempting to speculate that similar cellular processes may be involved in APP trafficking as well. In addition to Akt-dependent processes, atypical protein kinase C (aPKC) $\lambda\zeta$ is also involved in downstream GLUT4 trafficking (13,14). aPKCs can affect GLUT4 translocation to the plasma membrane by promoting association between the GTPase Rab4, motor proteins and microtubules required for GLUT4 translocation (35). It is possible that these pathways are involved in modulating APP trafficking as well.

Our studies and others have shown that inhibition of the insulin signaling pathway through direct PI3K inhibition or through feedback inhibition of PI3K decreased APP trafficking and secretion. It is unclear, however, how this inhibition of the insulin signaling pathway will alter APP trafficking *in vivo* and, if so, what consequences this will have on AD progression. Intracellular accumulation of sAPPs, APP, and Aβ may invoke negative consequences. Secreted sAPPs, in particular sAPPα, have been suggested to be neuroprotective and may also play a mitogenic role (36–38); therefore, decreased secretion of sAPPs could render cells more vulnerable to toxic insults associated with AD, if sAPPs are indeed protective. In addition, some have hypothesized that intracellular accumulation of Aβ could promote toxicity or disrupt intracellular signaling pathways (39). Other studies suggest the Aβ could aggregate within the acidic environment of endosomes that when secreted could actually seed amyloid aggregation reactions and promote plaque formation (40). Therefore, both a decrease in extracellular sAPPs and an increase in intracellular Aβ could produce pathogenic consequences.

This study suggests that overactivation of the insulin signaling pathway may initiate a feedback inhibition pathway that results in reduced IRS1 levels and inhibition of PI3K. PI3K inhibition negatively regulates APP secretion, resulting in abnormal accumulation of secreted APPs and Aβ within the cell. Further studies are necessary to determine the mechanism of how PI3K regulates APP trafficking and to determine what consequences this negative regulation of APP secretion will produce *in vivo* in terms of disease progression.

Acknowledgments

We acknowledge Dr. Morris Birnbaum (University of Pennsylvania) for providing reagents and fruitful advice. We thank Dr. Peter Klein (University of Pennsylvania) for constructive review and helpful comments.

References

1. Koo EH, Squazzo SL. Evidence that production and release of amyloid beta-protein involves the endocytic pathway. J Biol Chem 1994;269:17386–17389. [PubMed: 8021238]
2. Mattson MP. Pathways towards and away from Alzheimer's disease. Nature 2004;430:631–639. [PubMed: 15295589]
3. Vetrivel KS, Thinakaran G. Amyloidogenic processing of {beta}-amyloid precursor protein in intracellular compartments. Neurology 2005;XX

4. Ling Y, Morgan K, Kalsheker N. Amyloid precursor protein (APP) and the biology of proteolytic processing: relevance to Alzheimer's disease. Int J Biochem Cell Biol 2003;35:1505–1535. [PubMed: 12824062]
5. Hardy J. A hundred years of Alzheimer's disease research. Neuron 2006;52:3–13. [PubMed: 17015223]
6. Sisodia SS. Beta-amyloid precursor protein cleavage by a membrane-bound protease. Proc Natl Acad Sci U SA 1992;89:6075–6079.
7. Yan R, Han P, Miao H, Greengard P, Xu H. The transmembrane domain of the Alzheimer's beta-secretase (BACE1) determines its late Golgi localization and access to beta-amyloid precursor protein (APP) substrate. J Biol Chem 2001;276:36788–36796. [PubMed: 11466313]
8. Kinoshita A, Fukumoto H, Shah T, Whelan CM, Irizarry MC, Hyman BT. Demonstration by FRET of BACE interaction with the amyloid precursor protein at the cell surface and in early endosomes. J Cell Sci 2003;116:3339–3346. [PubMed: 12829747]
9. Chyung JH, Raper DM, Selkoe DJ. Gamma-secretase exists on the plasma membrane as an intact complex that accepts substrates and effects intramembrane cleavage. J Biol Chem 2005;280:4383–4392. [PubMed: 15569674]
10. Annaert WG, Levesque L, Craessaerts K, Dierinck I, Snellings G, Westaway D, George-Hyslop PS, Cordell B, Fraser P, De Strooper B. Presenilin 1 controls gamma-secretase processing of amyloid precursor protein in pre-Golgi compartments of hippocampal neurons. J Cell Biol 1999;147:277–294. [PubMed: 10525535]
11. Chyung AS, Greenberg BD, Cook DG, Doms RW, Lee VMY. Novel beta-secretase cleavage of beta-amyloid precursor protein in the endoplasmic reticulum/intermediate compartment of NT2N cells. J Cell Biol 1997;138:671–680. [PubMed: 9245794]
12. Taniguchi CM, Emanuelli B, Kahn CR. Critical nodes in signalling pathways: insights into insulin action. Nat Rev Mol Cell Biol 2006;7:85–96. [PubMed: 16493415]
13. Farese RV, Sajan MP, Standaert ML. Atypical protein kinase C in insulin action and insulin resistance. Biochem Soc Trans 2005;33:350–353. [PubMed: 15787604]
14. Welsh GI, Hers I, Berwick DC, Dell G, Wherlock M, Birkin R, Leney S, Tavare JM. Role of protein kinase B in insulin-regulated glucose uptake. Biochem Soc Trans 2005;33:346–349. [PubMed: 15787603]
15. Gasparini L, Gouras GK, Wang R, Gross RS, Beal MF, Greengard P, Xu H. Stimulation of beta-amyloid precursor protein trafficking by insulin reduces intraneuronal beta-amyloid and requires mitogen-activated protein kinase signaling. J Neurosci 2001;21:2561–2570. [PubMed: 11306609]
16. Solano DC, Sironi M, Bonfini C, Solerte SB, Govoni S, Racchi M. Insulin regulates soluble amyloid precursor protein release via phosphatidyl inositol 3 kinase-dependent pathway. FASEB J 2000;14:1015–1022. [PubMed: 10783157]
17. Adlerz L, Holback S, Multhaup G, Iverfeldt K. IGF-1-induced processing of the amyloid precursor protein family is mediated by different signaling pathways. J Biol Chem 2007;282:10203–10209. [PubMed: 17301053]
18. Petanceska SS, Gandy S. The phosphatidylinositol 3-kinase inhibitor wortmannin alters the metabolism of the Alzheimer's amyloid precursor protein. J Neurochem 1999;73:2316–2320. [PubMed: 10582589]
19. Forman MS, Cook DG, Leight S, Doms RW, Lee VMY. Differential effects of the swedish mutant amyloid precursor protein on beta-amyloid accumulation and secretion in neurons and nonneuronal cells. J Biol Chem 1997;272:32247–32253. [PubMed: 9405428]
20. Gravina SA, Ho L, Eckman CB, Long KE, Otvos L Jr, Younkin LH, Suzuki N, Younkin SG. Amyloid beta protein (A beta) in Alzheimer's disease brain. Biochemical and immunocytochemical analysis with antibodies specific for forms ending at A beta 40 or A beta 42(43). J Biol Chem 1995;270:7013–7016. [PubMed: 7706234]
21. Wertkin AM, Turner RS, Pleasure SJ, Golde TE, Younkin SG, Trojanowski JQ, Lee VMY. Human neurons derived from a teratocarcinoma cell line express solely the 695-amino acid amyloid precursor protein and produce intracellular beta-amyloid or A4 peptides. Proc Natl Acad Sci USA 1993;90:9513–9517. [PubMed: 8415732]

22. Turner RS, Suzuki N, Chyung AS, Younkin SG, Lee VMY. Amyloids beta40 and beta42 are generated intracellularly in cultured human neurons and their secretion increases with maturation. J Biol Chem 1996;271:8966–8970. [PubMed: 8621541]

23. Lee EB, Zhang B, Liu K, Greenbaum EA, Doms RW, Trojanowski JQ, Lee VMY. BACE overexpression alters the subcellular processing of APP and inhibits Abeta deposition in vivo. J Cell Biol 2005;168:291–302. [PubMed: 15642747]

24. Nagoshi T, Matsui T, Aoyama T, Leri A, Anversa P, Li L, Ogawa W, del Monte F, Gwathmey JK, Grazette L, Hemmings BA, Kass DA, Champion HC, Rosenzweig A. PI3K rescues the detrimental effects of chronic Akt activation in the heart during ischemia/reperfusion injury. J Clin Invest 2005;115:2128–2138. [PubMed: 16007268]

25. Gual P, Marchand-Brustel Y, Tanti JF. Positive and negative regulation of insulin signaling through IRS-1 phosphorylation. Biochimie 2005;87:99–109. [PubMed: 15733744]

26. Hers I, Tavare JM. Mechanism of feedback regulation of insulin receptor substrate-1 phosphorylation in primary adipocytes. Biochem J 2005;388:713–720. [PubMed: 15713122]

27. Harrington LS, Findlay GM, Lamb RF. Restraining PI3K: mTOR signalling goes back to the membrane Trends. Biochem Sci 2005;30:35–42.

28. Aguirre V, Uchida T, Yenush L, Davis R, White MF. The c-Jun NH(2)-terminal kinase promotes insulin resistance during association with insulin receptor substrate-1 and phosphorylation of Ser(307). J Biol Chem 2000;275:9047–9054. [PubMed: 10722755]

29. Li Y, Soos TJ, Li X, Wu J, Degennaro M, Sun X, Littman DR, Birnbaum MJ, Polakiewicz RD. Protein kinase C Theta inhibits insulin signaling by phosphorylating IRS1 at Ser(1101). J Biol Chem 2004;279:45304–45307. [PubMed: 15364919]

30. Gao Z, Hwang D, Bataille F, Lefevre M, York D, Quon MJ, Ye J. Serine phosphorylation of insulin receptor substrate 1 by inhibitor kappa B kinase complex. J Biol Chem 2002;277:48115–48121. [PubMed: 12351658]

31. Mothe I, Van Obberghen E. Phosphorylation of insulin receptor substrate-1 on multiple serine residues, 612, 632, 662, and 731, modulates insulin action. J Biol Chem 1996;271:11222–11227. [PubMed: 8626671]

32. Ravichandran LV, Esposito DL, Chen J, Quon MJ. Protein kinase C-zeta phosphorylates insulin receptor substrate-1 and impairs its ability to activate phosphatidylinositol 3-kinase in response to insulin. J Biol Chem 2001;276:3543–3549. [PubMed: 11063744]

33. Chang Q, Li Y, White MF, Fletcher JA, Xiao S. Constitutive activation of insulin receptor substrate 1 is a frequent event in human tumors: therapeutic implications. Cancer Res 2002;62:6035–6038. [PubMed: 12414625]

34. Bellacosa A, Testa JR, Staal SP, Tsichlis PN. A retroviral oncogene, akt, encoding a serine-threonine kinase containing an SH2-like region. Science 1991;254:274–277. [PubMed: 1833819]

35. Imamura T, Huang J, Usui I, Satoh H, Bever J, Olefsky JM. Insulin-induced GLUT4 translocation involves protein kinase C-lambda-mediated functional coupling between Rab4 and the motor protein kinesin. Mol Cell Biol 2003;23:4892–4900. [PubMed: 12832475]

36. Furukawa K, Sopher BL, Rydel RE, Begley JG, Pham DG, Martin GM, Fox M, Mattson MP. Increased activity-regulating and neuroprotective efficacy of alpha-secretase-derived secreted amyloid precursor protein conferred by a C-terminal heparin-binding domain. J Neurochem 1996;67:1882–1896. [PubMed: 8863493]

37. Stein TD, Anders NJ, DeCarli C, Chan SL, Mattson MP, Johnson JA. Neutralization of transthyretin reverses the neuroprotective effects of secreted amyloid precursor protein (APP) in APPSW mice resulting in tau phosphorylation and loss of hippocampal neurons: support for the amyloid hypothesis. J Neurosci 2004;24:7707–7717. [PubMed: 15342738]

38. Caille I, Allinquant B, Dupont E, Bouillot C, Langer A, Muller U, Prochiantz A. Soluble form of amyloid precursor protein regulates proliferation of progenitors in the adult subventricular zone. Development 2004;131:2173–2181. [PubMed: 15073156]

39. Echeverria V, Cuello AC. Intracellular A-beta amyloid, a sign for worse things to come? Mol Neurobiol 2002;26:299–316. [PubMed: 12428762]

40. Skovronsky DM, Doms RW, Lee VMY. Detection of a novel intraneuronal pool of insoluble amyloid beta protein that accumulates with time in culture. J Cell Biol 1998;141:1031–1039. [PubMed: 9585420]

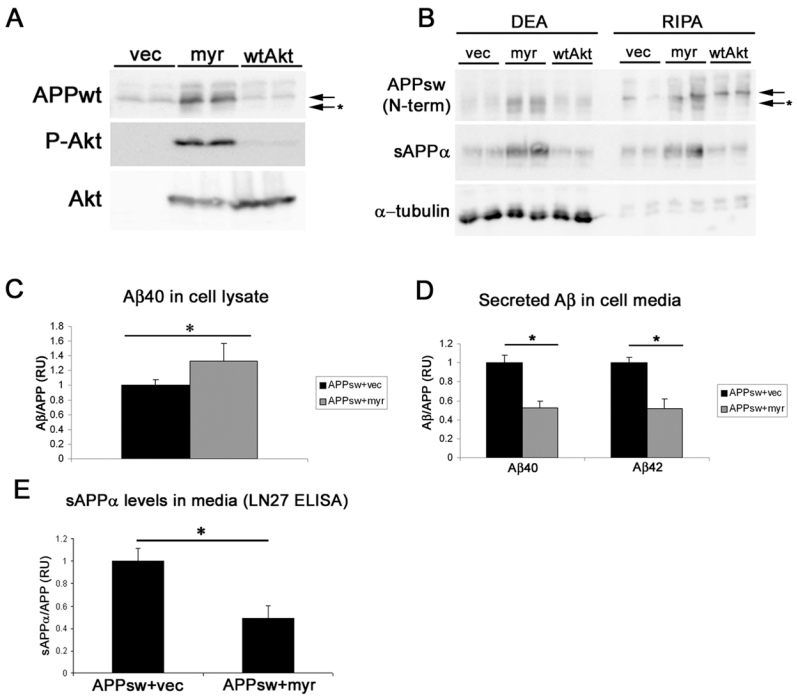

Figure 1.

Myr-Akt expression increases APP levels and decreases secretion of APP metabolites. Constitutively active Akt (myr-Akt) or wild-type Akt (wtAkt) was coexpressed with wild-type APP (APPwt) in QBI293 cells. Coexpression of empty vector (vec) is used as a control. (A) Western blot analysis for APP shows that myr-Akt increases APP levels (upper arrow) as well as a lower molecular weight species (starred arrow) that immunoreacts with an APP N-terminal antibody. Phospho-Akt and Akt Western blots are shown to verify expression and increased Akt activity with myr-Akt overexpression. (B) QBI293 cells transfected with Swedish mutant APP (APPsw) and either myr-Akt or wtAkt were sequentially extracted with DEA, to extract soluble material, followed by RIPA, to extract detergent-soluble material. Western blot of cell lysate for APP (upper arrow) and sAPPα (starred arrow) is shown. α-Tubulin is shown as a loading control. (C) A*β* ELISA of RIPA lysate from transfected cells shows increased intracellular A*β*40 levels with myr-Akt overexpression. (D) A*β* ELISA of conditioned media shows decreased secreted A*β*40 and A*β*42 with myr-Akt expression. (E) sAPPα ELISA of conditioned media shows decreased sAPPα levels with myr-Akt expression. ELISA data shown in (C), (D), and (E) are normalized to full-length APP quantified from Western blot analysis and represent pooled data from at least three separate experiments. Data expressed as mean ± SD. * = $p < 0.05$.

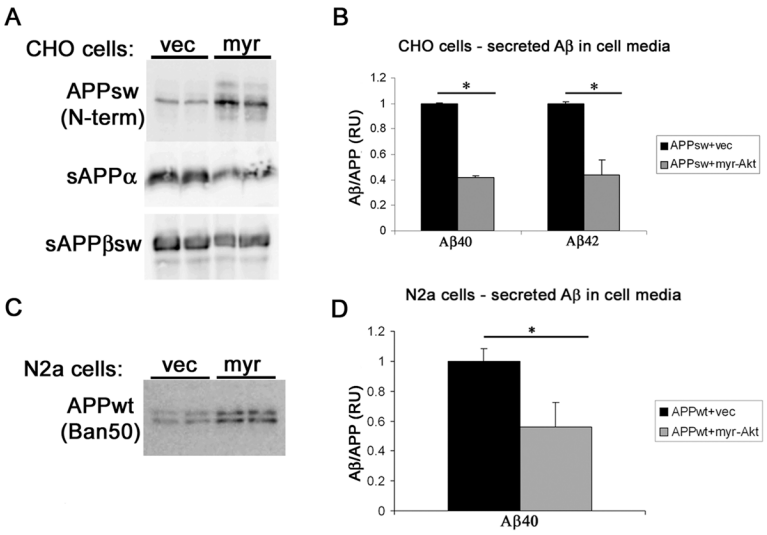

Figure 2.

Effects of myr-Akt expression on APP occur across multiple cell lines. (A) Western blot analysis of CHO cells expressing APPsw and either empty vector (vec) or myr-Akt (myr) is shown. APPsw levels in cell lysate are increased with myr-Akt expression, while levels of sAPPα and sAPP*β*sw in conditioned media are decreased. (B) A*β* ELISA on conditioned media from CHO cells shows decreased secreted A*β*40 and A*β*42. (C) Western blot analysis of N2a cells expressing APPwt and either vec or myr-Akt is shown. APPwt levels, shown using human-specific Ban50 antibody, are increased with myr-Akt expression. (D) A*β* ELISA of conditioned media shows decreased secreted A*β*40 with myr-Akt expression. ELISA data shown in (B) and (D) are normalized to full-length APP quantified from Western blot analysis and represent pooled data from at least three separate experiments. Data expressed as mean ± SD. * = $p < 0.05$.

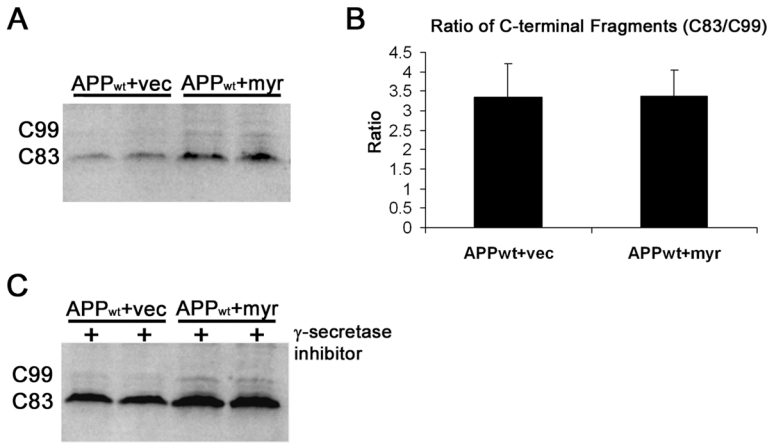

Figure 3.

Myr-Akt expression does not significantly alter cleavage of APP. (A) QBI293 cells were transfected with APPwt and either empty vector (vec) or myr-Akt (myr). Western blot analysis of the *β*-cleaved C-terminal fragment of APP (C99) and α-cleaved fragment (C83) is shown. (B) Quantitation of the ratio of C83/C99 demonstrates no significant difference between cells expressing vec and myr-Akt. (C) QBI293 cells were treated overnight with 1 *μ*M *γ*-secretase inhibitor X. Western blot analysis of C99 and C83 in cells expressing APPwt and either vec or myr-Akt is shown. Western blots shown in (A) and (C) are representative experiments.

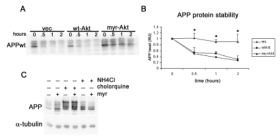

Figure 4.

Myr-Akt expression increases APP protein stability through reduced lysosomal degradation. QBI293 cells were transfected with APPwt and either vec, wt-Akt, or myr-Akt. (A) Western blot of APP levels at indicated time points following cyclohexamide treatment is shown. Quantitation from Western blots of three independent experiments is shown in (B). Myr-Akt expression significantly increases APP protein stability. (C) Western blot analysis of APP levels with or without myr-Akt expression and/or 18 h lysosomal inhibitor treatment (NH_4Cl or chloroquine). Representative Western blot is shown.

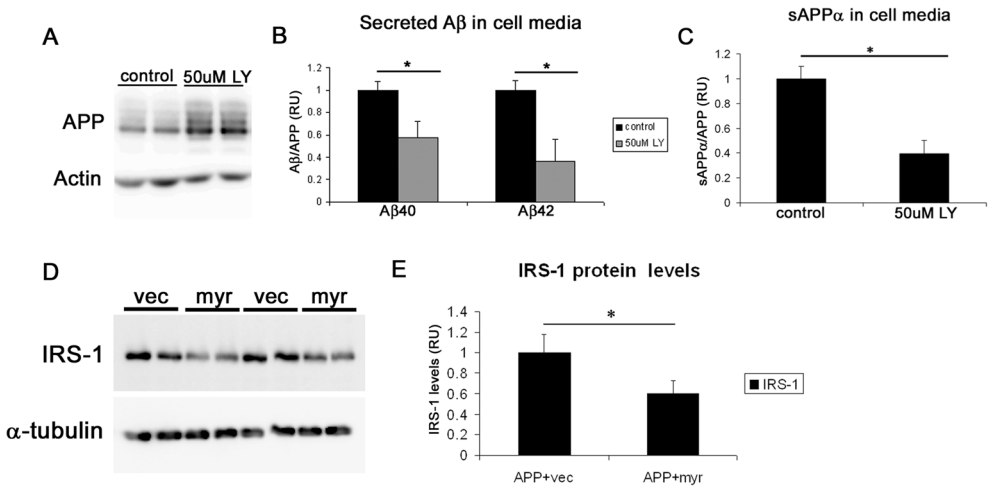

Figure 5.

Myr-Akt overexpression may act through feedback inhibition of PI3K to alter APP trafficking. (A) Western blot analysis of APP levels in QBI293 cells following 24 h treatment with PI3K inhibitor, LY-294002 (LY). Actin Western blot is shown as a loading control. (B) Aβ ELISA of conditioned media shows decreased Aβ40 and Aβ42 levels following LY treatment. (C) sAPPα levels in conditioned media following LY treatment were quantified from Western blot analysis. Data in (B) and (C) are normalized to full-length APP quantified from Western blot analysis and represent pooled data from at least three separate experiments. (D) Western blot analysis of IRS1 protein levels shows a statistically significant reduction with myr-Akt expression. α-Tubulin Western blot is shown as a loading control. Data are quantified from Western blots and graphed in (E) and represent pooled data from at least three separate experiments. Data are expressed as mean ± SD. * = $p < 0.05$.

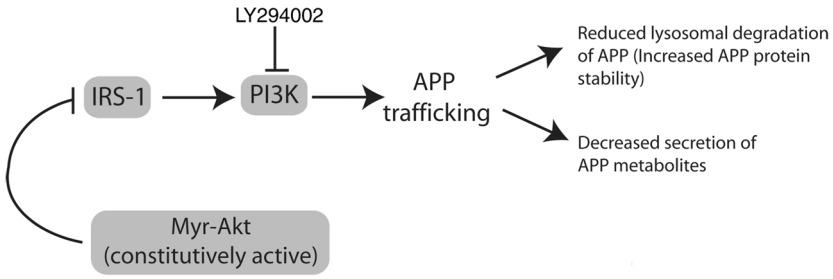

Figure 6.

Model: Effects of myr-Akt on APP trafficking and secretion may be mediated through IRS1-dependent feedback inhibition of PI3K. We hypothesize that constitutive Akt activation increases APP levels by impairing lysosomal degradation of APP and decreases secretion of Aβ and sAPPs. Reduced vesicular trafficking of APP can explain both of these phenomena. Our studies suggest that chronic Akt activation causes feedback inhibition of insulin/IGF1 signaling by decreasing IRS1 protein levels. This reduction in IRS1 levels inhibits PI3K activation, resulting in reduced trafficking of APP and APP metabolites.